ASME Journal of Mechanical Design
Online journal at:
https://asmedigitalcollection.asme.org/mechanicaldesign

Maximum Stress Minimization Via Data-Driven Multifidelity Topology Design

Misato Kato
Department of Mechanical Engineering,
Osaka University,
Suita, Osaka 565-0871, Japan
e-mail: kato@syd.mech.eng.osaka-u.ac.jp

Taisei Kii
Department of Mechanical Engineering,
Osaka University,
Suita, Osaka 565-0871, Japan
e-mail: kii@syd.mech.eng.osaka-u.ac.jp

Kentaro Yaji[1]
Department of Mechanical Engineering,
Osaka University,
Suita, Osaka 565-0871, Japan
e-mail: yaji@mech.eng.osaka-u.ac.jp

Kikuo Fujita
Department of Mechanical Engineering,
Osaka University,
Suita, Osaka 565-0871, Japan
e-mail: fujita@mech.eng.osaka-u.ac.jp

The maximum stress minimization problem is among the most important topics for structural design. The conventional gradient-based topology optimization methods require transforming the original problem into a pseudo-problem by relaxation techniques. Since their formulation methods and the parameter settings significantly influence optimization, a method is required to accurately solve the original maximum stress minimization problem without using relaxation techniques. This paper focuses on this challenge and compares solutions obtained by gradient-based topology optimization with those obtained by solving the original maximum stress minimization problem without relaxation techniques. We employ data-driven multifidelity topology design (MFTD), a gradient-free topology optimization based on evolutionary algorithms. The basic framework involves generating candidate solutions by solving a low-fidelity optimization problem, evaluating these solutions through high-fidelity forward analysis, and iteratively updating them using a deep generative model without sensitivity analysis. In this study, data-driven MFTD incorporates the optimized designs obtained by solving a gradient-based topology optimization problem with the p-norm stress measure in the initial solutions and solves the original maximum stress minimization problem based on a high-fidelity analysis with a body-fitted mesh. We demonstrate the effectiveness of our proposed approach through the benchmark of L-bracket. As a result of solving the original maximum stress minimization problem with data-driven MFTD, a volume reduction of up to 22.6% was achieved under the same maximum stress value, compared to the initial solution. [DOI: 10.1115/1.4067750]

Keywords: maximum stress minimization, data-driven design, design optimization, multiobjective optimization, topology optimization

1 Introduction

Topology optimization, which aims to derive the best structure by optimizing material distribution within the design domain to maximize performance, is increasingly adopted in various industrial applications [1,2]. While mean compliance minimization is predominant, stress-based topology optimization is actively researched for engineering applications [3,4].

Several methods have been proposed to effectively solve the maximum stress minimization problem. However, conventional methods still face numerical and practical challenges. As for the numerical challenge, several relaxation techniques are needed to effectively solve the maximum stress minimization and constraint problems using gradient-based methods. This is because stress-based topology optimization typically faces three challenges: singularity, strong nonlinearity, and stress localization [5]. Singularity problems arise in density-based topology optimization, which prevent nonlinear programming algorithms from searching for the optimal solution and cause convergence to the local optima [6–10]. To avoid this phenomenon, several techniques have been proposed to relax the stress values, such as ϵ-relaxation methods [11] and qp-relaxation methods [12,13]. Next, the maximum stress minimization problem is highly nonlinear and has many locally optimal solutions due to the multimodality of the solution space, making it difficult to search globally using the gradient-based methods. Furthermore, there are challenges related to the local nature of stress evaluation points. The computational burden increases with stress evaluation points in each element, which must be reduced by stress aggregation functions such as the p-norm and the Kreisselmeier–Steinhauser functions [14,15]. Therefore, to solve the maximum stress minimization problem using gradient-based methods, it is necessary to transform the original problem into a pseudo-problem using various relaxation techniques. These relaxation techniques cannot accurately capture the stress behavior, and the optimization results are highly sensitive to their parameters. Next, from a practical perspective, the intermediate state of the design variable, i.e., grayscale is a significant concern. Gradient-based methods require that all design variables must be relaxed with continuous variables through relaxation techniques. Since grayscale is an intermediate material between solid and void, it is difficult to interpret in engineering terms and the boundaries of the optimized results are ambiguous. It must generally be removed in the design process. In addition, density-based topology

[1]Corresponding author.

Contributed by Design Automation Committee of ASME for publication in the Journal of Mechanical Design. Manuscript received July 16, 2024; final manuscript received January 14, 2025; published online February 26, 2025. Assoc. Editor: Julián Norato.

optimization typically uses a structured mesh to compute the objective function. It results in staircase-like boundaries in the optimized structure [16,17], which can lead to stress concentrations at these edges. As a result, after optimization, the designer must perform post-processing steps such as binarization and smoothing, and re-analysis using a body-fitted mesh. These steps can significantly degrade performance and cause issues such as stress concentrations, often requiring considerable time investment to achieve manufacturable designs with desirable performance. It is necessary to achieve optimization based on stress analysis using 0/1 design variables and a body-fitted mesh.

To radically overcome the above challenges, gradient-free optimization is a promising option to deal with the 0/1 design variable field. Topology optimization methods using evolutionary algorithms (EAs) such as genetic algorithms [18] are the representative gradient-free method [19] and have been proposed in several research [20–24]. They can perform global search even in strongly nonlinear problems. However, EA-based topology optimization generally increases the computational burden with an increase in design variables, namely, the *curse of dimensionality*, and requires a large number of function calls of the forward analysis. In general, only a few hundred design variables can be handled, which is very small compared to typical cases in gradient-based topology optimization.

As a new approach to achieve gradient-free optimization without compromising the design freedom of topology optimization, Yaji et al. [25] proposed a gradient-free topology optimization framework called *data-driven multifidelity topology design (MFTD)*. The framework combines multifidelity design guided by topology optimization [26] with data-driven topology design [27], where the solutions are updated based on EAs. The fundamental concept is that candidate designs are generated by solving low-fidelity topology optimization problems, their objective functions are evaluated by high-fidelity forward analysis, and iteratively updated without gradient information until the desired solutions are obtained. The design updates are achieved by a deep generative model that corresponds to crossover in EAs. Data-driven MFTD has been shown to be applicable to topology optimization problems that are difficult to solve directly with conventional gradient-based methods, such as minimax [28,29] and turbulent flow problems [25]. The maximum stress minimization problem has been addressed by Yamasaki et al. [27]. However, there have not been sufficient discussions of the specific challenges inherent in this problem and the effectiveness of the framework in addressing those challenges. As a preliminary study, we have discussed the issue of the maximum stress minimization problem employing a pixel-based model for high-fidelity stress analysis [28]. From a practical point of view, it is necessary to evaluate the maximum stress values using a body-fitted mesh.

Therefore, this paper focuses on the challenges of the maximum stress minimization problem faced by conventional methods and investigates whether solutions with more avoided stress concentrations can be obtained by solving the original maximum stress minimization problem based on data-driven MFTD, compared to the solutions obtained by conventional methods. In this paper, "fidelity" is defined as the accuracy of the maximum stress value. A low-fidelity problem is a pseudo-problem that incorporates relaxation techniques such as intermediate density, approximate processing, and a structured mesh, which are typically handled by conventional gradient-based methods. On the other hand, a high-fidelity problem is an original problem that deals with the maximum value of the true stress obtained by forward analysis using black-and-white design and a body-fitted mesh. Specifically, we first generate several design solutions by gradient-based topology optimization using the p-norm, as a low-fidelity optimization. These solutions are then used as the initial solutions of the proposed framework, and they are iteratively updated based on a high-fidelity evaluation using an original maximum stress minimization problem to improve their performance. To improve the convergence of data-driven MFTD, this paper incorporates latent crossover, a method recently proposed by Kii et al. to efficiently perform crossover in the latent space of [29]. Through numerical examples, we discuss the challenges of the conventional method and the effectiveness of data-driven MFTD for the maximum stress minimization problem.

2 Problem Settings

In gradient-based topology optimization, the maximum stress minimization problem is usually defined as a volume-constrained single-objective optimization problem. Since EA-based optimization methods can naturally deal with multi-objective optimization problems, we consider the bi-objective optimization of maximum stress minimization and volume minimization as the original problem.

Figure 1(*a*) shows the L-bracket widely used as a benchmark for maximum stress minimization problems. Ω and $D \setminus \Omega$ denote the material and void domains in the design domain D, respectively. The material domain Ω is designed inside a pre-fixed design space D. The structure is fixed on Γ_D and $\boldsymbol{t}$ is the surface force applied on Γ_N. Since the initial structure concentrates stress at the reentrant corner, the material in this area is aggressively removed during optimization to reduce the maximum stress.

Let us consider the continuous form of a maximum stress minimization problem. A formulation of the bi-objective optimization problem can be defined by

$$\begin{aligned} &\text{find} && \Omega \subseteq D \\ &\text{that minimize} && \sigma_{\max} = \max\{\sigma_{\mathrm{vm}}(\boldsymbol{x}) \mid \forall \boldsymbol{x} \in \Omega\} \\ & && V = \int_{\Omega} d\Omega \end{aligned} \tag{1}$$

Herein σ_{vm} is the von Mises stress and $\boldsymbol{x}$ is the point inside the material domain Ω. Note that Eq. (1) deals with the maximum value of the true stress. Since the maximum stress is not differentiable, density-based methods cannot solve this original problem directly and must transform it into a pseudo-problem using relaxation techniques. The conventional formulation using the relaxation techniques is described in Sec. 3.

The analysis domain is typically discretized using the finite element method to calculate the evaluation functions. In density-based optimization, a structured mesh is commonly used as shown in Fig. 1(*b*). However, since the optimized structure depends on the shape of the mesh and stress concentration occurs at the edges, it is not suitable for the evaluation of maximum stress values. In this paper, we calculate the evaluation function in Eq. (1) using a body-fitted mesh as shown in Fig. 1(*c*), which is necessary to more accurately evaluate the maximum stress.

3 Conventional Approach

In gradient-based topology optimization, it is necessary to transform the original problem into a pseudo-problem using various relaxation techniques to solve the maximum stress minimization problem. In this section, we introduce general relaxation techniques and formulation using these techniques. Although there are several gradient-based methods, this study deals with the density-based method due to its design freedom and ease of implementation.

We discuss the general density-based topology optimization for solving the maximum stress minimization problem. Based on a finite element analysis using a structured mesh and the solid isotropic material with penalization (SIMP) [7,8,11,30], we defined a pseudo-density $\rho \in [0, 1]$ at each element as the design variable.

3.1 Density Filter. To avoid a checkerboard pattern and control the minimum length-scale, the SIMP method introduces the density filter [31,32] for the design variable ρ_i as follows:

$$\tilde{\rho}_i = \frac{\sum_{j \in \Omega_i} w_j \rho_i}{\sum_{j \in \Omega_i} w_j}, \quad i = 1, 2, \ldots, n \tag{2}$$

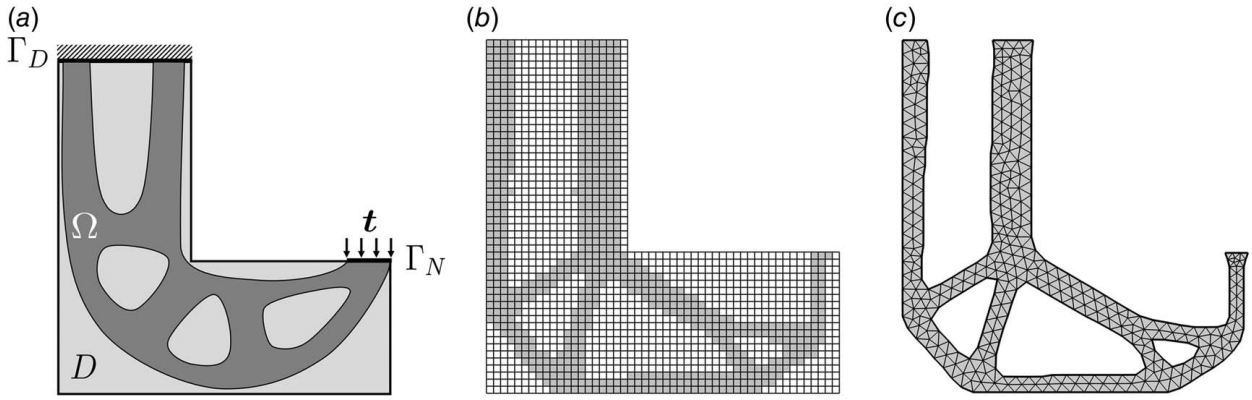

Fig. 1 Problem settings for L-bracket: (*a*) design domain *D* and the shape Ω, (*b*) discretization with structured mesh, and (*c*) discretization with body-fitted mesh

where Ω_i is in the influence domain of the element i. The weight factor w_j is calculated at each element j inside Ω_i as follows:

$$w_j = \frac{r_0 - r_j}{r_0} \tag{3}$$

where r_0 is the filter radius and r_j is the distance between the center points of each elements i and j. The density filter can control the minimum length-scale, and avoid mesh-dependence and stress concentration due to small and sharp structures.

In gradient-based topology optimization, it is common to use a combination of the density filter and the projection methods [33]. However, in this study, the projection method is not used to ensure numerical stability and solution diversity based on a result of preliminary validation.

3.2 Equilibrium Equation. Under the assumption of linear elasticity and static behavior, the discrete form of the equilibrium equation can be represented as $\boldsymbol{Ku} = \boldsymbol{F}$. $\boldsymbol{K}$ can be adequately built by using the stiffness matrix of an element $\boldsymbol{K}_i$ and the modified Young's modulus E_{SIMP}, given by

$$\begin{aligned} \boldsymbol{K} &= \sum_{i=1}^{n} E_{\text{SIMP}}(\tilde{\rho}_i)\boldsymbol{K}_i \\ E_{\text{SIMP}}(\tilde{\rho}_i) &= E_{\min} + \tilde{\rho}_i^p (E_0 - E_{\min}) \end{aligned} \tag{4}$$

where E_0 and $E_{\min}$ are Young's modulus of the solid ($\tilde{\rho}_i = 1$) and void ($\tilde{\rho}_i = 0$) phases, respectively. $E_{\min}$ is a small positive real number to avoid numerical instabilities. And p is the penalization parameter to promote binarization to achieve black-and-white designs finally. Typically, $p = 3$ is often used in topology optimization problems concerning the maximum stress minimization or constraint, as with the mean compliance [3,5,34].

3.3 Stress Relaxation. It is widely known that maximum stress minimization problems face a singularity problem, in which nonlinear programming algorithms cannot reach degenerate regions of the design space that often contain global optimum, and converges to a local solution [5]. Specifically, stress at the void could increase rapidly as one or more of the design variables tends to be zero. Hence, stress relaxation methods that smooth the design space are necessary to avoid singularity and stabilize the optimization process. Various stress relaxation methods have been proposed, e.g., the ε-relaxation and smooth envelope functions [11,35]. In this study, we use the *qp*-parameterization [5,12,34], one of the general relaxation methods.

The vector of stress at evaluation point i can be written in Voigt notation [34,36] as

$$\boldsymbol{\sigma}_i = (\sigma_{ix}\ \sigma_{iy}\ \sigma_{iz}\ \tau_{ixy}\ \tau_{iyz}\ \tau_{izx})^T \tag{5}$$

The penalized and relaxed stress measure $\hat{\boldsymbol{\sigma}}_i$ interpolating stress values for intermediate density is given as

$$\begin{aligned} \hat{\boldsymbol{\sigma}}_i(\tilde{\rho}_i) &= \eta(\tilde{\rho}_i)\boldsymbol{\sigma}_i \\ \eta(\tilde{\rho}_i) &= \tilde{\rho}_i^q \end{aligned} \tag{6}$$

where q is the penalization parameter, typically $q = 0.5$ is used [5,34]. This method also has the effect of penalizing intermediate values of the material density and promoting binarization. In addition, the following holds for both extreme values:

$$\hat{\boldsymbol{\sigma}}_i(\tilde{\rho}_i = 1) = \boldsymbol{\sigma}_i \tag{7}$$

$$\hat{\boldsymbol{\sigma}}_i(\tilde{\rho}_i = 0) = \lim_{\tilde{\rho}_i \to 0} \hat{\boldsymbol{\sigma}}_i(\tilde{\rho}_i) = 0 \tag{8}$$

Herein, Eq. (8) justifies that the *qp*-parameterization can avoid the singularity problem [37].

3.4 *P*-Norm Stress Measure. In this study, the relaxed von Mises stress of Eq. (6) is used as the stress measure in the optimization procedure. In the optimization problem (Eq. (1)), we replace the objective function expressed as the maximum stress with $\sigma_{\max} = \max_i(\hat{\sigma}_{\text{vm},i})$.

The maximum stress is not differentiable, so typically it needs to be approximated using a global function in gradient-based methods. We use p-norm stress measure given by

$$\sigma_{\text{PN}} = \left(\sum_{i=1}^{n} \hat{\sigma}_{\text{vm},i}^P \right)^{1/P} \tag{9}$$

Herein, the p-norm σ_{PN} approaches the maximum stress $\sigma_{\max}$ when the parameter $P \to \infty$, whereas numerical computation becomes impossible. Therefore, a finite value is used for P, but the larger the value of P, the greater the numerical instability. Thus, the optimization highly depends on the selection of this parameter, and it is necessary to select an appropriate value for the stress norm parameter P that provides good search performance and numerical stability. In previous works, although $P = 8$ was often chosen from the viewpoint of numerical stability during optimization [5], it cannot accurately capture the maximum stress. In this paper, we employ the continuation method [2] to achieve both a large P setting and numerical stability. It allows numerical stability by increasing the stress norm parameter P at every predetermined interval during optimization. The effectiveness of this method is discussed in Sec. 5.

3.5 Problem Formulation. In this study, the original optimization problem of Eq. (1) has two objectives: maximum stress minimization and volume minimization. To solve this bi-objective

problem using the conventional gradient-based topology optimization methods, we use the ε-constraint approach [38,39] to replace the problem with a single objective optimization problem, the volume-constrained maximum stress minimization problem. Consequently, the optimization problem can be formulated as follows:

$$\begin{aligned} &\text{find} && \boldsymbol{\rho} = \rho_i\,(i = 1, 2, \ldots, n) \\ &\text{that minimize} && \sigma_{\mathrm{PN}} = \left(\sum_{i=1}^{n} \hat{\sigma}_{\mathrm{vm},i}^{P} \right)^{1/P} \\ &\text{subject to} && V = \sum_{i=1}^{n} v_i \rho_i \le \overline{V} \le V_{\max} \\ & && \rho_i \in [0, 1] \end{aligned} \tag{10}$$

where v_i is the element i solid volume, $\overline{V}$ is the volume constraint, and $V_{\max}$ is the design domain volume. Herein, Eq. (10), which includes several relaxation techniques, can be defined as a pseudo-problem compared to the original optimization problem of Eq. (1). We solve this optimization problem by using the method of moving asymptotes (MMA) [40], one of the popular gradient-based optimizer in the research community of topology optimization.

4 Proposed Approach

In this study, we tackle the original maximum stress minimization problem (Eq. (1)) based on data-driven MFTD [25] that is a gradient-free topology optimization framework under a high degree of design freedom. Specifically, we investigates whether optimized designs obtained by solving the optimization problem (Eq. (10)) which is handled by the conventional gradient-based method, can be improved on the original topology optimization problem (Eq. (1)). It should be emphasized that the proposed approach in this study is a framework for optimization that updates the solutions based on the results of high-fidelity stress analysis using a body-fitted mesh without the relaxation techniques used in gradient-based methods.

The procedures of data-driven MFTD are shown in Fig. 2. Each step is briefly described below. Note that this paper omits a mutation-like operation proposed in the original framework for simplicity and the detailed procedures can be found in the original paper [25].

4.1 Low-Fidelity Optimization. In contrast to the original problem to be solved, a pseudo-problem, i.e., a low-fidelity optimization problem, is defined. A pseudo-optimization problem incorporating design parameters, called seeding parameters, is solved by gradient-based topology optimization to generate a variety of design candidates. In this study, we use the relaxed problem formulation in Eq. (10) as the low-fidelity optimization problem and the seeding parameter is the volume constraint $\overline{V}$. Various patterns of initial designs for the framework are generated based on the ε-constraint method.

4.2 High-Fidelity Evaluation. In this step, all the candidates are evaluated by the high-fidelity model on the original objective space in Eq. (1), namely, the maximum von Mises stress $\sigma_{\max}$ and the volume fraction $V/V_{\max}$. It should be emphasized that the framework only requires the forward analysis of the original high-fidelity model without any gradient information on the objective and constraint functions.

The high-fidelity model treated here is a model as shown in Fig. 1(*c*), in which binarization, smoothing, and body-fitted mesh are applied to low-fidelity model represented by pixel as shown in Fig. 1(*b*). This allows the analysis on the original problem (Eq. (1)). Note that non-analyzable solutions such as discontinuities and non-generatable meshes are excluded from the candidate solutions.

4.3 Selection. Based on the results of the high-fidelity evaluation, superior candidates so-called elite solutions are selected from the candidate solutions using an elite strategy of EAs. In this study, the idea of the non-dominated sorting genetic algorithm II (NSGA-II), one of the representative selection algorithms, is used to rank and select candidates based on the Pareto dominance relation in the objective space [41]. Specifically, solutions with superior objectives and diversity are selected as training data for variational autoencoder (VAE) to generate the next candidate solutions based on the non-dominated sorting and the crowding distance sorting used as the selection algorithms commonly used in the NSGA-II. Based on the EA strategy, high-fidelity evaluation, selection, and generation of candidate solutions are repeated until the Pareto front converges.

4.4 Generative Model. The aim in this step is to generate new candidate solutions with the characteristics of the selected elite solutions in selection by using a generative model. The important point here is that the material distributions can be updated without sensitivity analysis. We use a VAE [42], which is one of the representative deep generative models. As shown in Fig. 2, a VAE consists of two neural networks, namely, an encoder and a decoder. It has the ability to extract the information from the high-dimensional input

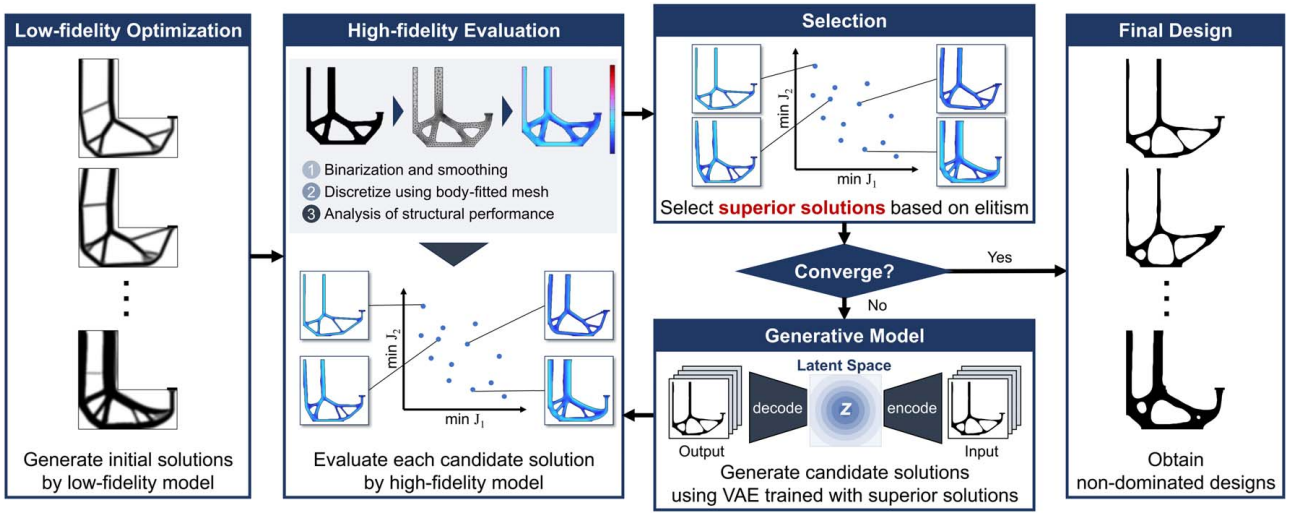

Fig. 2 Schematic illustration of data-driven multifidelity topology design

data, and to compressed it into a lower-dimensional manifold called latent space. In the standard VAE, the latent variable $\boldsymbol{z}$ is defined as

$$\boldsymbol{z} = \boldsymbol{\mu} + \boldsymbol{\sigma} \circ \boldsymbol{\varepsilon} \tag{11}$$

where $\boldsymbol{\mu}$ is the mean, $\boldsymbol{\sigma}$ is the variance, $\circ$ is the element-wise product, and $\boldsymbol{\varepsilon}$ is a random vector following the standard normal distribution. With this architecture, a VAE uses the same dataset for inputs and outputs to perform unsupervised learning to construct the latent space. The training dataset consists of the pixel-based material distributions of the elite solutions, i.e., a vector of design variables defined for each element of the structured mesh.

The following loss function L_{VAE} is used for learning [43]:

$$L_{\text{VAE}} = L_{\text{recon}} + \varrho L_{\text{KL}} \tag{12}$$

where L_{recon} is the reconstruction loss measured by the mean squared error, and L_{KL} is the Kullback–Leibler (KL) divergence. ϱ is the weight parameter that controls the influence of the KL divergence that works to regularize the latent field to be $N(0, 1)$. L_{KL} is given by

$$L_{\text{KL}} = -\frac{1}{2}\sum_{i=1}^{N_{\text{lt}}}\left(1 + \log(\sigma_i^2) - \mu_i^2 - \sigma_i^2\right) \tag{13}$$

where N_{lt} is the dimension of the latent space, μ_i and σ_i are the ith components of $\boldsymbol{\mu}$ and $\boldsymbol{\sigma}$, respectively.

In this way, it is expected to extract essential features of the training data by compressing high-dimensional input and output data into a low-dimensional latent space.

Consequently, by sampling from this latent space, candidate solutions with the characteristics of elite solutions are obtained as a vector of design variables. In this study, to reduce the randomness in sampling process, we employ latent crossover, a scheme for sampling candidates intensively from meaningful regions in the latent space [29].

5 Results and Discussion

In this section, we present numerical examples of a maximum stress minimization problem and demonstrate the challenges of conventional gradient-based topology optimization and the effectiveness of the proposed approach with data-driven MFTD.

In this study, we used COMSOL MULTIPHYSICS (version 6.1), a commercial software based on the finite element method to perform stress analysis for both low-fidelity optimization and high-fidelity evaluation. Additionally, the binarization and the application of the body-fitted mesh for generating the high-fidelity model were automated. From the perspective of computational cost and stability during automatic mesh generation, we used linear triangle elements for a body-fitted mesh as an initial step in this study. The VAE was implemented using PYTHON (version 3.9.12), and the overall loop for gradient-based topology optimization and data-driven MFTD was controlled using MATLAB (version 2022b).

5.1 Design Settings. We deal with the L-bracket shown in Fig. 3, which gives the dimensions, loads, and boundary conditions. All the constants are dimensionless values, and $L = 2$, $l = 0.2$, $h = 0.04$. To avoid stress concentration, the total force $F = 1$ applied to the top boundary of the non-design domain. The Young's modulus is set as $E_0 = 1$ for the solid and $E_{\min} = 10^{-9}$ for the void. Poisson's ratio is $\nu = 0.3$ and the filter radius is $r_0 = 0.05$. The 2D solid element considering plane stress state is employed. Based on preliminary investigations, we set 25,600 elements for the structured mesh in the low-fidelity model, balancing computational cost and the accuracy of the body-fitted mesh. For high-fidelity model, the body-fitted mesh is applied to each solution.

5.2 Generation of Initial Solutions. We generate various design candidates by adjusting the volume constraints $\overline{V}/V_{\max}$ from 0.2 to 0.5 in 0.05 increments. The discrete adjoint method [34,44] is used for sensitivity analysis to derive gradient information, and the MMA is used as the gradient-based optimizer [40]. The convergence criterion is simply set to the maximum iteration of 200. The move limit of the MMA is set to 0.05.

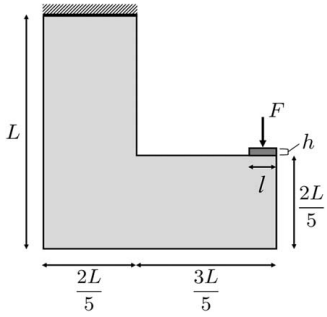

Fig. 3 Boundary conditions and dimensions for L-bracket

In order to verify whether there is room for improvement in the optimized designs obtained by the conventional method, it is necessary to prepare the best initial solutions as much as possible. Therefore, we employ the continuation method for the parameter P of p-norm stress measure to obtain solutions with more avoided stress concentrations. First, we test the effectiveness of the continuation method, in which P is increased every 30 steps as 8–16–32 by comparing the solutions obtained using the fixed stress norm parameter $P = 8$.

Figure 4 shows the effect of the continuation method on the maximum von Mises stress with the stress distributions of the solutions. Here, the maximum von Mises stress is the maximum value of the relaxed stress $\sigma_{\max} = \max_i(\hat{\sigma}_{\text{vm},i})$ defined as Eq. (6). The results indicate that the continuation method achieves a better

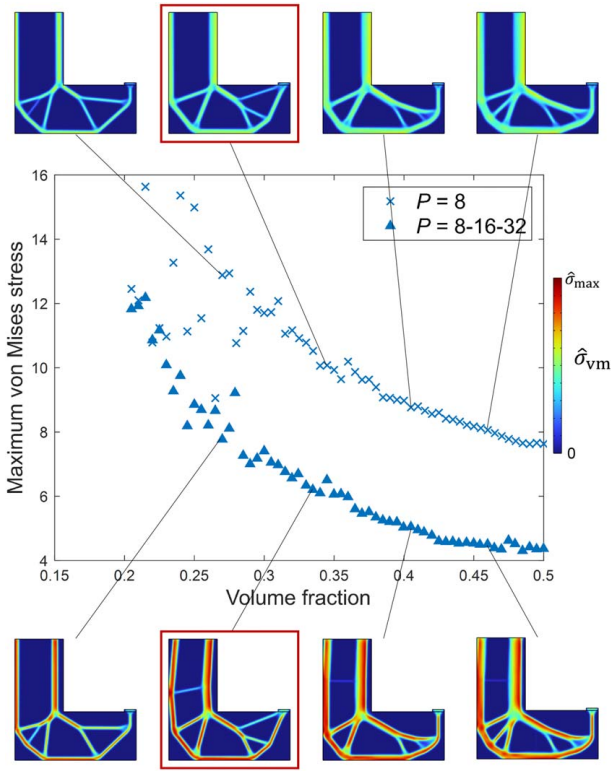

Fig. 4 Effect of the continuation method on the objective space of the relaxed maximum von Mises stress $\max(\hat{\sigma}_{\text{vm}})$ and volume fraction $V/V_{\max}$ with the stress distributions of the solutions

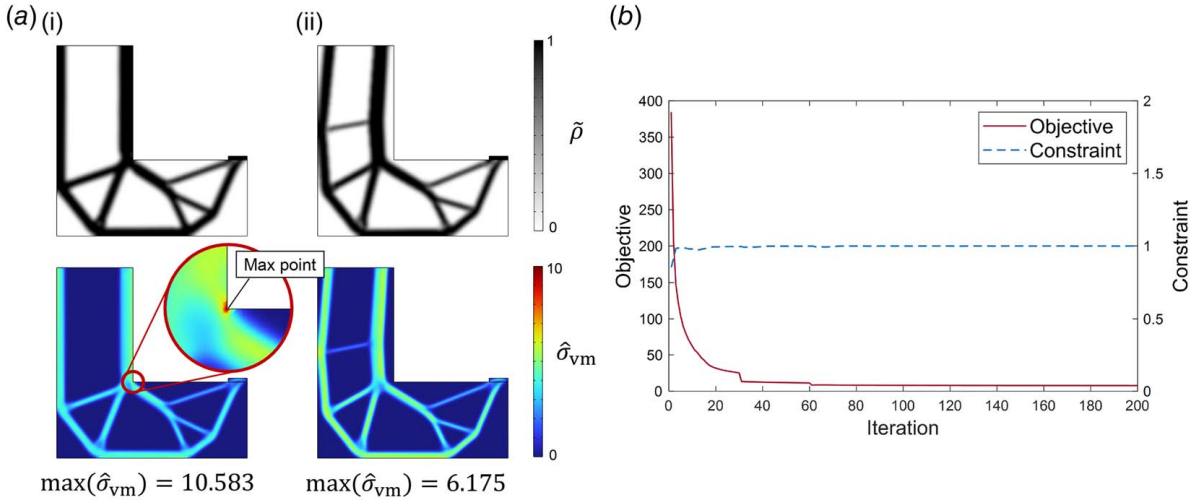

Fig. 5 (*a*) Optimized designs with the filtered density $\tilde{\rho}$ and their stress distributions in the same volume constraint $\overline{V}/V_{max} = 0.335$ under (i) the fixed parameter $P = 8$ and (ii) the continuation method $P = 8 - 16 - 32$; (*b*) convergence history of the objective function and the normalized volume constraint in the low-fidelity optimization using the continuation method $P = 8 - 16 - 32$

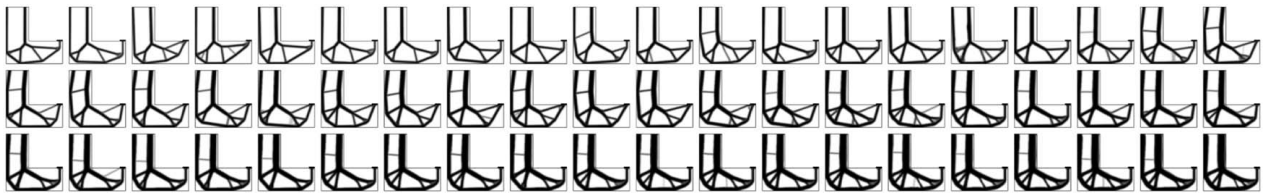

Fig. 6 Initial solutions for data-driven MFTD generated by the low-fidelity optimization using the continuation method $P = 8 - 16 - 32$

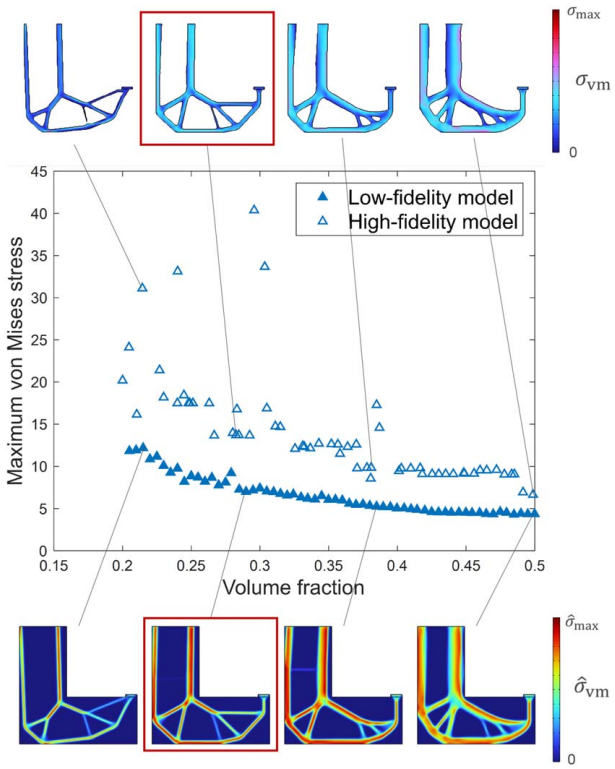

Fig. 7 Effect of the fidelity on the objective space of the maximum von Mises stress σ_{max} and volume fraction V/V_{max}, in which each stress value indicates the relaxed stress max($\hat{\sigma}_{vm}$) (bottom: low-fidelity model) and the true stress max(σ_{vm}) (top: high-fidelity model), respectively

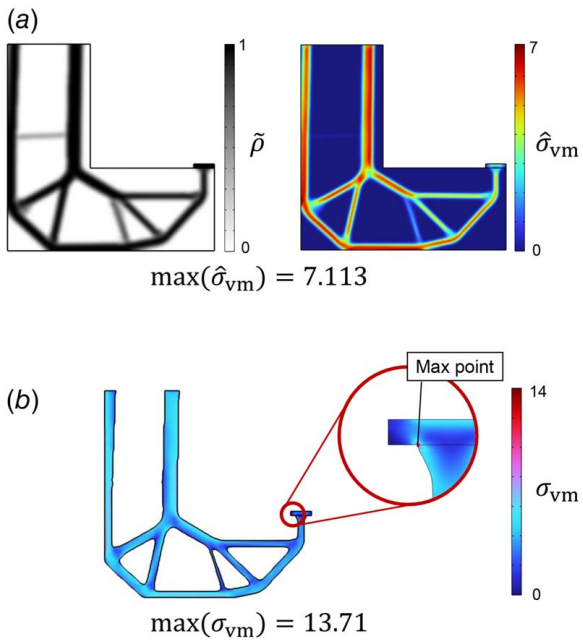

Fig. 8 Optimized design and its stress distribution in different analysis model: (*a*) the low-fidelity model with the filtered density $\tilde{\rho}$ and (*b*) the high-fidelity model

Pareto front and obtained the solutions with a more uniform stress distribution compared with the $P = 8$ fixed case. Figure 5 shows the optimized designs and their stress distributions in the same volume constraint $\overline{V}/V_{max} = 0.335$ under the fixed parameter $P = 8$ and the continuation method $P = 8 - 16 - 32$, which are the same

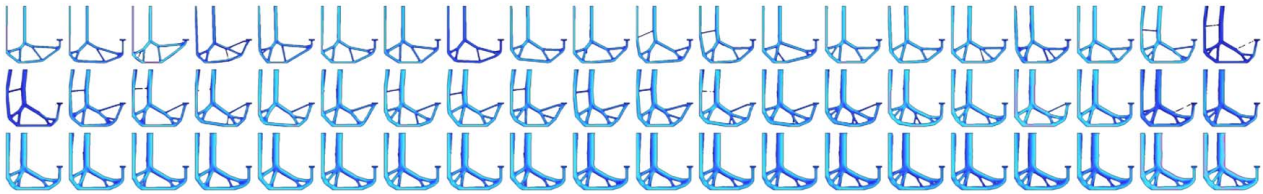

Fig. 9 Initial solutions analyzed with the high-fidelity model

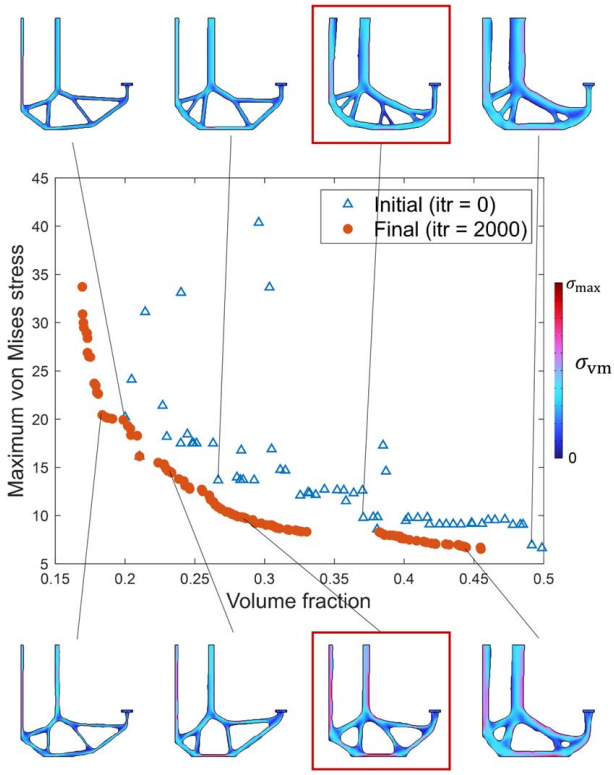

Fig. 10 Objective space with initial and final designs

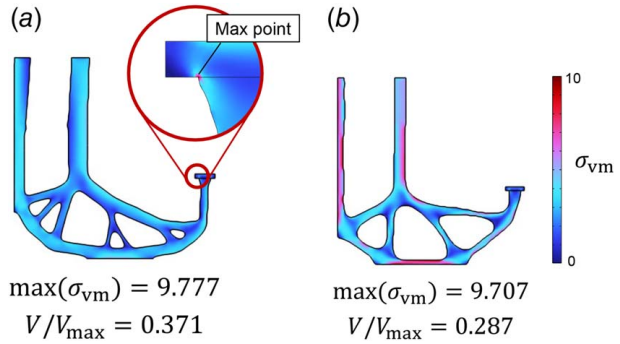

Fig. 11 (*a*) An initial solution and (*b*) a final solution with almost the same maximum stress value

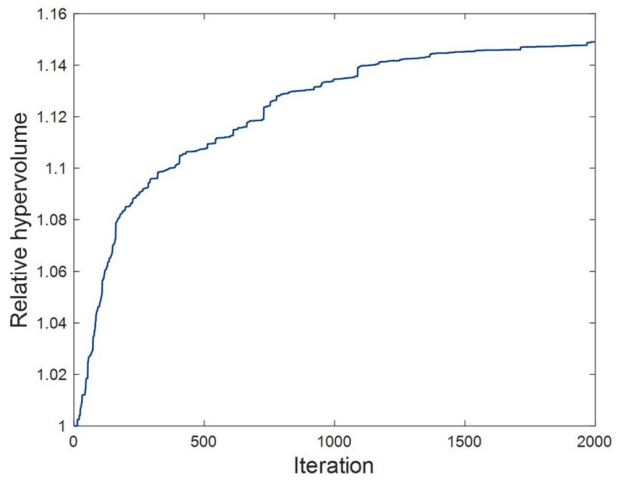

Fig. 12 Convergence history of the hypervolume indicator

solutions shown by the box in Fig. 4. The reentrant corner of a solution under $P = 8$ is filled with the material as shown in Fig. 5(*a*) (i), causing stress concentrations, while the continuation method more accurately captures the maximum, hence material in this area is actively removed and stress concentrations are relaxed as shown in Fig. 5(*a*) (ii). Therefore, this method can avoid such a singularity problem. Figure 5(*b*) shows the convergence history of the objective function and the normalized volume constraint for the solution under the continuation method $P = 8 - 16 - 32$ shown in Fig. 5(*a*) (ii). The objective function here is the p-norm stress measure defined as Eq. (9). As shown in Fig. 5(*b*), the objective and constraint functions converge well enough in all solutions, and it can be said that, at least under the investigated conditions, the gradient-based topology optimization method with the continuation method has resulted in optimized structures. Note that the sudden drops in the objective function history at 30 and 60 iterations are due to the p-norm continuation method. In the formulation of the maximum stress minimization problem, the p-norm function only needs to capture the trend of the maximum stress, and the scale of the p-norm function itself is not critical.

From the above, we adopt the continuation method in low-fidelity optimization and use 60 optimized designs as the initial designs for data-driven MFTD. Figure 6 shows the optimized designs of them. Here, let us focus on the structure of the obtained results. As shown in Fig. 6, various structures appear even when the volumes are close to each other. At first glance, there is no clear relationship between structural changes and volume increases, and the number of members also varies. However, very similar structures can be observed even when the volumes differ.

Next, Fig. 7 shows the effect of the fidelity of the analysis model on the maximum von Mises stress. The result for the low-fidelity model shows the maximum relaxed stress of the solutions obtained by low-fidelity optimization, which is the same as the result for the continuation method $P = 8 - 16 - 32$ in Fig. 4. On the other hand, the result for the high-fidelity model shows the maximum values of the true stress obtained through analyzing them after post-processing and discretization with a body-fitted mesh. As shown in Fig. 7, the maximum stress exhibits significant variability. This is due to stress concentrations resulting from structural changes caused by post-processing, in addition to the difference in stress indices. Figure 8 shows the optimized design and its stress distribution in different analysis model, the low-fidelity and high-fidelity models. Post-processing has resulted in the disappearance of members composed of intermediate densities, and the structure has also changed. In the low-fidelity model as shown in Fig. 8(*a*), stress is almost uniformly distributed throughout the whole

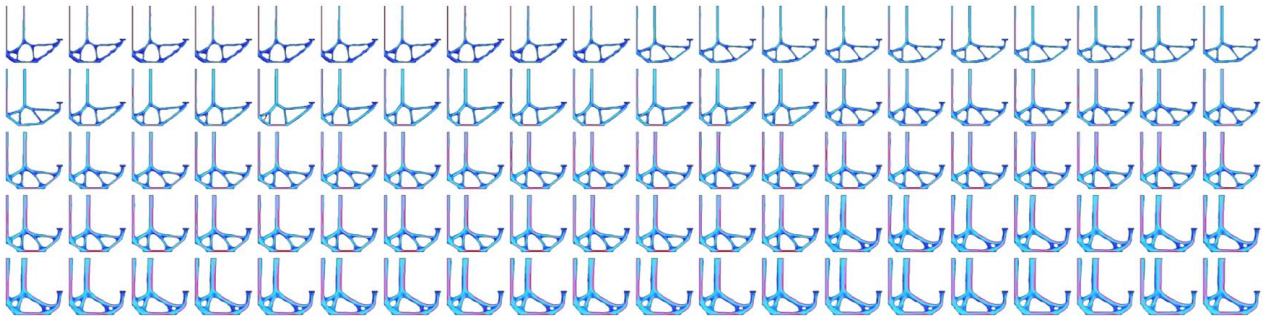

Fig. 13 Final solutions by data-driven MFTD

structure, whereas in the high-fidelity model as shown in Fig. 8(*b*), stresses are concentrated locally at a single point in the loading area, and the maximum stress values are different. Figure 9 shows the stress distribution of all designs ordered by decreasing volume. It can be noticed that stresses are concentrated locally in most of the solutions and some designs have disconnected members. It should be emphasized that this is a serious problem in actual design because it is difficult to predict the variations in stress values due to the fidelity of the analysis model.

5.3 Improvement of Pareto Solutions. This study investigates the potential enhancement of performance in designs optimized through the gradient-based topology optimization method by applying further optimization using data-driven MFTD. It aims to demonstrate the efficacy of the gradient-free approach for the maximum stress minimization problem.

The initial solutions obtained in Fig. 6 is input to data-driven MFTD to produce the Pareto solutions. Then, we tackle to solve the original optimization problem (Eq. (1)) based on high-fidelity stress analysis. The convergence criterion is the maximum iteration number of 2000, after which the solutions were considered to be converged. Here, at each optimization step, 100 elite solutions survive and are trained by a VAE, after which 100 new candidate solutions are generated. The architecture of the VAE is a simple neural network based on a multilayer perceptron with one hidden layer each for the encoder and decoder. In this study, the number of neurons in the input/output and hidden layers is 25,600 and 512, respectively. For the latent space, the mean $\boldsymbol{\mu}$, the variance $\boldsymbol{\sigma}$, and the latent variable $\boldsymbol{z}$ are structured on 8 neurons.

Figure 10 shows the objective space with the stress distribution of some initial and final solutions. The Pareto front has been progressed from the initial solutions, indicating that the conventional gradient-based topology optimization has room for improvement in terms of solving the original maximum stress minimization problem. Figure 11 shows the initial and final designs with almost the same maximum stress value, which are the same solutions shown by the box in Fig. 10. The objective function values are $\max(\sigma_{\mathrm{vm}}) = 9.777$ with $V/V_{\max} = 0.371$, and $\max(\sigma_{\mathrm{vm}}) = 9.707$ with $V/V_{\max} = 0.287$, respectively. Specifically, a volume reduction of 22.6% was achieved under almost the same stress value, compared to the initial solution. Focusing on the structures, it can be observed that the final solution as shown in Fig. 11(*b*) has fewer members and a simpler structure than the initial solution as shown in Fig. 11(*a*). Additionally, the solutions obtained by conventional gradient-based topology optimization are linear and uniform in member thickness. On the other hand, since there is no limit on the thickness of the members in data-driven MFTD, the final solution features more rounded holes and reentrant corner to relax stress compared to the initial solution. Furthermore, focusing on stress distributions, the initial solution has a localized concentration of stress, whereas the final solution has a more uniform stress distribution due to stress dispersion.

Figure 12 shows the convergence history of the hypervolume indicator which is a measure often used to assess the performance of multi-objective evolutionary algorithms [45]. In the case of two objective functions, it is represented by the area formed by the reference point and the Pareto front in the objective space. In this study, the reference point is the maximum values of the objective functions in the initial solutions. As shown in Fig. 12, the hypervolume gradually improves up to 2,000 iterations, indicating that the Pareto front continues to progress. Note that the number of iterations is relatively large compared to other optimization problems investigated in the original paper [25]. Figure 13 shows the final designs ordered by decreasing volume. It can be observed that the initial solutions are various structures depending on the volume, while the final solutions have a relatively similar topology. This result indicates that although the Pareto solutions are not necessarily the globally optimal, it can be expected that the comprehensive solution search via data-driven MFTD has yielded a promising topology among numerous local solutions. It can also be said that data-driven MFTD yielded superior solutions that could not be reached by the conventional method, since structures with more avoided stress concentrations were obtained that are not typically found in the gradient-based method.

To generate the data in Fig. 10, we run data-driven MFTD codes over a 2.2 GHz AMD Ryzen Threadripper PRO 3995WX 64-cores CPU. The VAE code was run on two NVIDIA RTX A2000 GPUs. One iteration of the data-driven MFTD takes 100 s. A large portion of the computational time is dedicated to high-fidelity evaluation, and the computational cost can be reduced through the effective promotion of parallelization.

6 Conclusion

In this paper, we focused on the remaining challenges of the maximum stress minimization problem solved by the standard gradient-based topology optimization method and proposed a new framework to overcome those challenges. To accurately solve the maximum stress minimization problem, we focused on data-driven MFTD, a gradient-free topology optimization method, and proposed an optimization framework based on high-fidelity stress analysis using a body-fitted mesh. This framework derived initial solutions by solving the gradient-based topology optimization using the p-norm stress measure, and they are updated by a VAE based on the manner of EAs, without using sensitivity analysis. It was confirmed that solutions with more avoided stress concentrations were obtained compared to the initial solutions obtained by the gradient-based method, as the Pareto front has been progressed by data-driven MFTD. The comprehensive solution search using data-driven MFTD for the original maximum stress minimization problem resulted in structures with characteristics not commonly seen in conventional methods, achieving designs with reduced stress concentrations. we also achieved to derive one promising topology among many local solutions.

The method is applicable to optimization problems where low-fidelity optimization problem can be formulated and the original problem can be evaluated by forward analysis in high-fidelity evaluation. As for future work, we consider that our framework can be

applied to further complex and practical optimization problems considering strong geometrical nonlinearity such as buckling and large deformations under the original maximum stress minimization or constraint problem.

Acknowledgment

This work was supported by JSPS KAKENHI Grant Nos. 23K26018 and 24KJ1639.

Conflict of Interest

There are no conflicts of interest.

Data Availability Statement

The datasets generated and supporting the findings of this article are obtainable from the corresponding author upon reasonable request.

References

[1] Bendsøe, M. P., and Kikuchi, N., 1988, "Generating Optimal Topologies in Structural Design Using a Homogenization Method," Comput. Methods Appl. Mech. Eng., **71**(2), pp. 197–224.
[2] Bendsøe, M. P., and Sigmund, O., 2004, *Topology Optimization:Theory, Methods, and Applications*, Springer, Berlin, Heidelberg.
[3] Duysinx, P., and Bendsøe, M. P., 1998, "Topology Optimization of Continuum Structures With Local Stress Constraints," Int. J. Numerical Methods Eng., **43**(8), pp. 1453–1478.
[4] Yang, D., Liu, H., Zhang, W., and Li, S., 2018, "Stress-Constrained Topology Optimization Based on Maximum Stress Measures," Comput. Struct., **198**(1), pp. 23–39.
[5] Le, C., Norato, J., Bruns, T., Ha, C., and Tortorelli, D., 2010, "Stress-Based Topology Optimization for Continua," Struct. Multidiscipl. Optim., **41**(4), pp. 605–620.
[6] Kirsch, U., 1990, "On Singular Topologies in Optimum Structural Design," Struct. Optim., **2**(3), pp. 133–142.
[7] Cheng, G., and Jiang, Z., 1992, "Study on Topology Optimization With Stress Constraints," Eng. Optim., **20**(2), pp. 129–148.
[8] Rozvany, G. I. N., 2001, "On Design-Dependent Constraints and Singular Topologies," Struct. Multidiscipl. Optim., **21**(2), pp. 164–172.
[9] Verbart, A., Langelaar, M., and Keulen, F. v., 2016, "Damage Approach: A New Method for Topology Optimization With Local Stress Constraints," Struct. Multidiscipl. Optim., **53**(5), pp. 1081–1098.
[10] Norato, J. A., Smith, H. A., Deaton, J. D., and Kolonay, R. M., 2022, "A Maximum-Rectifier-Function Approach to Stress-Constrained Topology Optimization," Struct. Multidiscipl. Optim., **65**(10), p. 286.
[11] Cheng, G. D., and Guo, X., 1997, "ϵ-Relaxed Approach in Structural Topology Optimization," Struct. Optim., **13**(4), pp. 258–266.
[12] Bruggi, M., 2008, "On An Alternative Approach to Stress Constraints Relaxation in Topology Optimization," Struct. Multidiscipl. Optim., **36**(2), pp. 125–141.
[13] Moon, S. J., and Yoon, G. H., 2013, "A Newly Developed QP-Relaxation Method for Element Connectivity Parameterization to Achieve Stress-Based Topology Optimization for Geometrically Nonlinear Structures," Comput. Methods Appl. Mech. Eng., **265**(1), pp. 226–241.
[14] Duysinx, P., and Sigmund, O., 1998, "New Developments in Handling Stress Constraints in Optimal Material Distribution".
[15] Yang, R. J., and Chen, C. J., 1996, "Stress-Based Topology Optimization," Struct. Optim., **12**(2), pp. 98–105.
[16] Liu, J., and Ma, Y., 2016, "A Survey of Manufacturing Oriented Topology Optimization Methods," Adv. Eng. Softw., **100**(1), pp. 161–175.
[17] Svärd, H., 2015, "Interior Value Extrapolation: A New Method for Stress Evaluation During Topology Optimization," Struct. Multidiscipl. Optim., **51**(3), pp. 613–629.
[18] Goldberg, D. E., 1989, *Genetic Algorithms in Search, Optimization, and Machine Learning*, Addison Wesley, New York.
[19] Coello, C. A. C., Lamont, G. B., and Veldhuizen, D. A. V., 2007, *Evolutionary Algorithms for Solving Multi-objective Problems*, Springer, New York.
[20] Wang, S. Y., and Tai, K., 2005, "Structural Topology Design Optimization Using Genetic Algorithms With a Bit-Array Representation," Comput. Methods Appl. Mech. Eng., **194**(36), pp. 3749–3770.
[21] Madeira, J. F. A., Pina, H. L., and Rodrigues, H. C., 2010, "GA Topology Optimization Using Random Keys for Tree Encoding of Structures," Struct. Multidiscipl. Optim., **40**(1), pp. 227–240.
[22] Zhou, H., 2010, "Topology Optimization of Compliant Mechanisms Using Hybrid Discretization Model," ASME J. Mech. Des., **132**(11), p. 111003.
[23] Guirguis, D., Aulig, N., Picelli, R., Zhu, B., Zhou, Y., Vicente, W., Iorio, F., Olhofer, M., Matusik, W., Coello, C. A. C., and Saitou, K., 2020, "Evolutionary Black-Box Topology Optimization: Challenges and Promises," IEEE Trans. Evol. Comput., **24**(4), pp. 613–633.
[24] Zhou, H., and Patil, R. B., 2012, "The Discrete Topology Optimization of Structures Using the Improved Hybrid Discretization Model," ASME J. Mech. Des., **134**(12), p. 124503.
[25] Yaji, K., Yamasaki, S., and Fujita, K., 2022, "Data-Driven Multifidelity Topology Design Using a Deep Generative Model: Application to Forced Convection Heat Transfer Problems," Comput. Methods Appl. Mech. Eng., **388**(1), p. 114284.
[26] Yaji, K., Yamasaki, S., and Fujita, K., 2020, "Multifidelity Design Guided by Topology Optimization," Struct. Multidiscipl. Optim., **61**(3), pp. 1071–1085.
[27] Yamasaki, S., Yaji, K., and Fujita, K., 2021, "Data-Driven Topology Design Using a Deep Generative Model," Struct. Multidiscipl. Optim., **64**(3), pp. 1401–1420.
[28] Kato, M., Kii, T., Yaji, K., and Fujita, K., 2023, "Tackling an Exact Maximum Stress Minimization Problem With Gradient-Free Topology Optimization Incorporating a Deep Generative Model," Proceedings of the International Design Engineering Technical Conferences and Computers and Information in Engineering Conference, Vol. 3B, p. V03BT03A008.
[29] Kii, T., Yaji, K., Fujita, K., Sha, Z., and Seepersad, C. C., 2024, "Latent Crossover for Data-Driven Multifidelity Topology Design," ASME J. Mech. Des., **146**(5), p. 051713.
[30] Rozvany, G. I. N., and Birker, T., 1994, "On Singular Topologies in Exact Layout Optimization," Struct. Optim., **8**(4), pp. 228–235.
[31] Bourdin, B., 2001, "Filters in Topology Optimization," Int. J. Numerical Methods Eng., **50**(9), pp. 2143–2158.
[32] Bruns, T. E., and Tortorelli, D. A., 2001, "Topology Optimization of Non-Linear Elastic Structures and Compliant Mechanisms," Comput. Methods Appl. Mech. Eng., **190**(26), pp. 3443–3459.
[33] Wang, F., Lazarov, B. S., and Sigmund, O., 2011, "On Projection Methods, Convergence and Robust Formulations in Topology Optimization," Struct. Multidiscipl. Optim., **43**(6), pp. 767–784.
[34] Holmberg, E., Torstenfelt, B., and Klarbring, A., 2013, "Stress Constrained Topology Optimization," Struct. Multidiscipl. Optim., **48**(1), pp. 33–47.
[35] Rozvany, G. I. N., and Sobieszczanski-Sobieski, J., 1992, "New Optimality Criteria Methods: Forcing Uniqueness of the Adjoint Strains by Corner-Rounding at Constraint Intersections," Struct. Optim., **4**(3), pp. 244–246.
[36] Kiyono, C. Y., Vatanabe, S. L., Silva, E. C. N., and Reddy, J. N., 2016, "A New Multi-p-norm Formulation Approach for Stress-Based Topology Optimization Design," Comp. Struct., **156**(1), pp. 10–19.
[37] Kočvara, M., and Stingl, M., 2012, "Solving Stress Constrained Problems in Topology and Material Optimization," Struct. Multidiscipl. Optim., **46**(1), pp. 1–15.
[38] Marler, R. T., and Arora, J. S., 2004, "Survey of Multi-objective Optimization Methods for Engineering," Struct. Multidiscipl. Optim., **26**(6), pp. 369–395.
[39] Miettinen, K., 1998, *Nonlinear Multiobjective Optimization*, Springer, New York.
[40] Svanberg, K., 1987, "The Method of Moving Asymptotes-A New Method for Structural Optimization," Int. J. Numerical Methods Eng., **24**(2), pp. 359–373.
[41] Deb, K., Pratap, A., Agarwal, S., and Meyarivan, T., 2002, "A Fast and Elitist Multiobjective Genetic Algorithm: NSGA-II," IEEE Trans. Evol. Comput., **6**(2), pp. 182–197.
[42] Kingma, D. P., and Welling, M., 2013, "Auto-Encoding Variational Bayes". arXiv preprint.
[43] Kingma, D. P., and Ba, J., 2014, "Adam: A Method for Stochastic Optimization". arXiv preprint.
[44] Nabaki, K., Shen, J., and Huang, X., 2019, "Stress Minimization of Structures Based on Bidirectional Evolutionary Procedure," J. Struct. Eng., **145**(2), p. 04018256.
[45] Shang, K., Ishibuchi, H., He, L., and Pang, L. M., 2021, "A Survey on the Hypervolume Indicator in Evolutionary Multiobjective Optimization," IEEE Trans. Evol. Comput., **25**(1), pp. 1–20.